IEEE Transactions on Nuclear Science, Vol.NS-25, No.1, February 1978

THE CHARACTERISTICS OF COMPUTED TOMOGRAPHIC RECONSTRUCTION NOISE AND THEIR EFFECT ON DETECTABILITY*

Kenneth M. Hanson
University of California
Los Alamos Scientific Laboratory
Los Alamos, NM 87545

Douglas P. Boyd
University of California, San Francisco
Department of Radiology
San Francisco, CA 94143

The process of reconstruction of a 2-D density distribution from 1-D projections has the effect of suppressing the low frequency portions of the noise power spectral density distribution. This low frequency suppression is demonstrated for computed tomographic (CT) reconstructions from an EMI 5005 scanner. An alternative method of displaying the implied long range negative correlation in CT noise is through the noise granularity function. It is expected that large objects are easier to detect in the presence of computed tomographic noise than in the presence of white noise of the same r.m.s. magnitude. A simple detectability phantom is described which allows this hypothesis to be tested on x-ray CT scanners.

Introduction

Riederer, Pelc and Chesler[1] have brought attention to the fact that the noise found in computed tomographic(CT) reconstructions may have some rather unusual properties. Indeed, if the noise in the input projections is uncorrelated, i.e. white, the noise in the resulting CT reconstruction will possess long-range negative correlations. These negative correlations arise from the suppression of the low frequency content of the input projections. Thus, if CT noise is spatially averaged over a circle of diameter d, the variance in the averaged values will drop faster than d^{-2}, which is the case for white noise. Hanson[2] has shown that the above statements are true for reconstructions produced from projections containing simulated white noise. In this paper we will show that they also hold for the reconstructions from at least one commercial x-ray scanner, the EMI 5005.

It would be desirable to have a quantitative measure for the dose efficiency of CT scanners based on the relationship between the noise in the reconstructions to the dose delivered to the patients. The foregoing comments indicate that such a figure of merit may not be easily reached, especially when one considers the variety of spatial smoothing that may be used in the reconstruction process. The ultimate goal of the CT image is to provide visual information to the radiologist. Thus it is important to understand the effect of the unusual properties of CT noise on the observation performance of the radiologists. To that end we will describe a phantom designed to measure the detectability of various sized circles on x-ray scanners.

Noise Granularity Function

Boyd, Korobkin and Moss[3] introduced the application of the noise granularity function[4] to CT images as a method of summarizing the dependence of the noise upon spatial averaging. The noise granularity is defined as the r.m.s. deviation of the mean noise averaged over an area A multiplied by the square root of the area. For white noise the noise granularity remains constant as A is varied. Figure 1 shows the noise granularity dependence upon $\sqrt{A}$ for a CT reconstruction from projections containing simulated white noise. A single 256 x 256 reconstruction was produced from 300 projections using the filtered backprojection algorithm. The solid lines were computed using square averaging areas for the two filters cited. The slope of these curves for $\sqrt{A}$ greater than 4 pixels is -0.30. The dashed curve shows the effect of using a pyramidal weighting in the averaging of the ramp filter reconstruction. Its slope is -0.50 as one would expect from the noise power spectrum to be discussed later.

Figure 2 displays the noise granularity function obtained from six reconstructions for the EMI 5005 scanner. The error bars shown on the data points indicate the one standard deviation statistical uncertainty in their values. The uniformity in the reconstructions was extremely good since the EMI water calibration was used. Earlier results[3] did not show the reduction in the noise granularity above 4 pixels, presumably due to slight nonuniformities in the reconstructions used. It should be noted that in Figure 2 a pixel refers to one element in the 320 x 320 data matrix generated by the EMI machine. There is a striking similarity between the data points and the granularity curve of Figure 1 for the sinc^2 filter function.

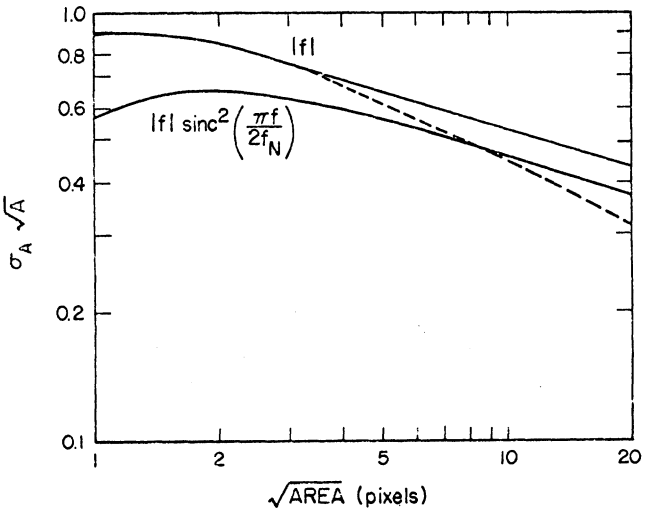

Figure 1

Noise granularity function for CT reconstructions from simulated data using two reconstruction filters. The solid line results from averaging over square regions with a constant weight whereas the dashed line results from a pyramidal weighting function. f_N is the Nyquist frequency.

*This work was supported in part through funding by the United States Energy and Research Administration.

0018-9499/78/0200-0160$00.75

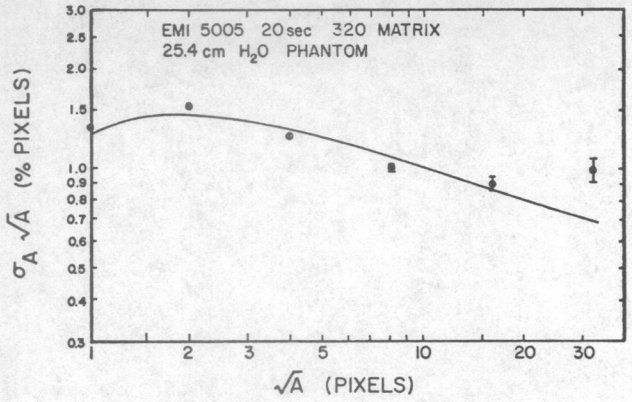

Figure 2

Noise granularity obtained from 6 reconstructuions of a water calibration phantom by the EMI 5005. The solid curve is the noise granularity from simulated data using the $sinc^2$ filter.

- - - - - - - -

Noise Power Spectrum

The noise power spectrum (NPS) presents more detailed information about the noise than the granularity function. The noise power spectral density may be defined as the ensemble average of the square of the Fourier transform of images containing pure noise. The ensemble average represents the average overall images containing the same type of noise. It has been shown[2] that the noise power spectral density S which results from the CT reconstruction by the filtered backprojection algorithm using white noise projection data has the form

$$S \sim |f||h(f)|^2\sigma_p^2 \qquad (1)$$

where σ_p^2 is the noise variance in the projections data and the filter used in reconstruction is $|f|h(f)$. Noise power spectra were calculated from a single 256 x 256 reconstruction using 300 simulated projections for two different reconstruction filters. The radial frequency dependences of the calculated NPS are shown in Figure 3 together with their predicted behavior, the dashed curves. The wiggles in the calculated curves arise from the finite statistics used in the calculation. The calculated curves are filled in at the origin and rounded off before the Nyquist frequency, $(2 \times \text{sample spacing})^{-1}$, as a result of the smoothing performed in frequency space in order to smooth out the statistical fluctuations. Otherwise, the calculated curves agree well with the predictions.

The noise granularity function may be expressed in terms of the NPS since the noise variance in the smoothed image is simply the total power:

$$\sigma^2 = \iint df_x df_y \; S(f_x,f_y) \; |H(f_x,f_y)|^2 \qquad (2)$$

where H is the effective filter corresponding to the spatial smoothing performed. When the noise granularity is calculated on the basis of square averaging areas, H is nearly the product of sinc factors with arguments f_x and f_y. It is not quite this because of the discrete nature of the image presented in pixels. Thus H is really the discrete Fourier transform of the averaging function. If H^2 falls off fast enough, faster than $|f|^{-2}$, then $\sigma\sqrt{A} \sim A^{-1/4}$ as is the case with the pyramidal weighting, Figure 2. For constant weighting

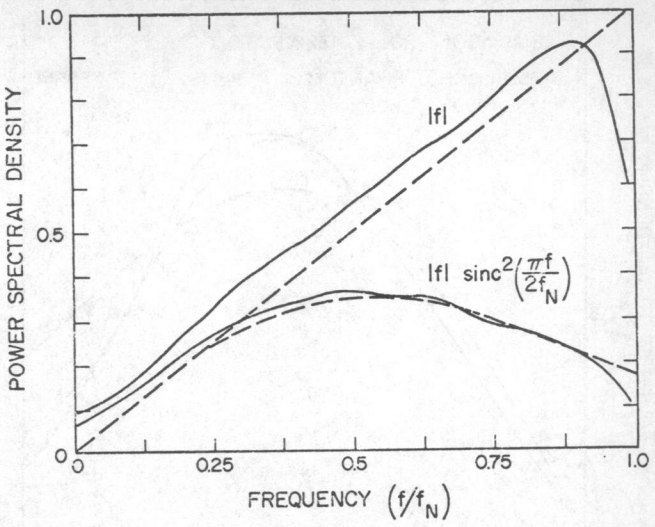

Figure 3

Noise power spectra of CT reconstructions from simulated data using two reconstruction filters. The dashed lines show the dependence predicted by Eq. 1.

- - - - - - - -

within square regions, H^2 does not fall off fast enough for this to hold.

The two dimensional noise power spectrum obtained from a single reconstruction of the water calibration phantom by the EMI 5005 is shown in Figure 4. This NPS is reasonably symmetric indicating an even contribution to the noise from all angles. Figure 5 shows the average radial frequency dependence of the NPS obtained from two EMI 5005 images. The two NPS were the same to within 10%. The EMI NPS is very linear up to 0.4 f_N with the exception of the small bump at zero frequency. This bump could be caused by low frequency artifacts, for example due to beam hardening calibration errors. Above 0.4 f_N the NPS starts to all away from the ramp function, peaking near 0.6 f_N. It is seen that the NPS for a $sinc^2$ reconstruction filter does not fit the EMI curve well, although it has generally the same features. Thus we conclude that the noise granularity function, which was seen in Figure 2 to agree with the $sinc^2$ filter fairly well, is not as sensitive to the reconstruction filter as is the noise power spectrum. A much better fit to the measured NPS is the dash-dotted curve in Figure 5 which corresponds to a reconstruction

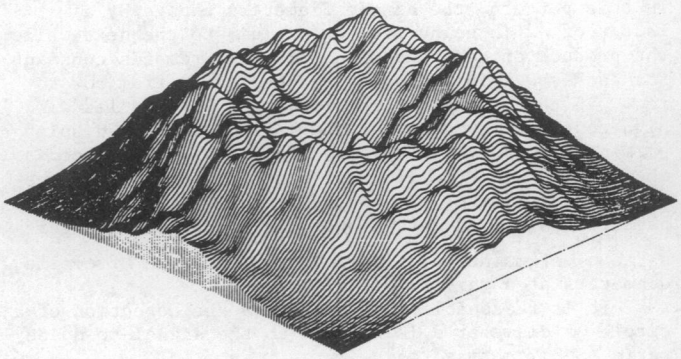

Figure 4

The two dimensional noise power spectrum for reconstructions from the EMI 5005 scanner.

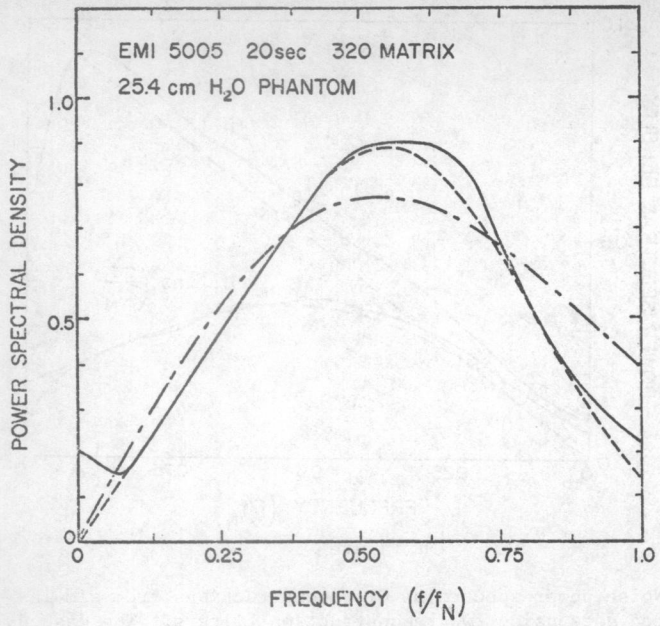

Figure 5

Noise power spectrum for EMI 5005 scanner. The dash-dotted curve shows the expected dependence for a $|f|\mathrm{sinc}^2(\frac{\pi f}{2f_N})$ reconstruction filter. The dashed curve shows the dependence for a filter with a Hanning taper as described in the text.

- - - - - - - -

that is constant up to 0.4 f_N and then falls off as a Hanning function, $1/2(1 + \cos X)$, to its half value at 0.86 f_N.

Detectability

In the clinical situation it is frequently required that the radiologist detect some anomoly in the radiograph or CT image presented to him. Ultimately it would be desirable to determine the efficacy of each CT scanner in this detection task. As an intermediate step it is interesting to determine the capability of human observers to detect the presence of various-sized circles on a flat background in the presence of CT noise.

A detectability pattern, Figure 6, has been developed[2] which permits this kind of determination over a wide range of circle sizes with relatively few images. In this pattern, the circle diameters change by a factor of $\sqrt{2}$ in going from one column to the next while the product of contrast times diameter remains constant for each row. This product changes by $\sqrt{2}$ from row to row. In the display of this pattern, the circles with high contrast may saturate the latitude of the display element, however, the "window" can usually be placed so the circles near the limit of detection are within the operating region of the display. This detectability pattern has the advantage over the traditional Burger pattern[5] of maintaining a wide dynamic range of circle diameters at a variety of noise levels.

It is reasonable to expect that the detection of a circle of diameter d is related to the signal-to-noise ratio (SNR), defined as

$$\mathrm{SNR} = \frac{C}{\sigma_d} \qquad (3)$$

where C is the contrast of the circle relative to the background and σ_d is the r.m.s. deviation of the noise averaged over a circular region of diameter d. Indeed, it has been found that in images containing white noise the threshold SNR for human observers remains constant over a wide range of circle sizes.[6] The noise granularity function is related to the SNR. We might expect, assuming a constant SNR threshold, that the product of the threshold contrast times $\sqrt{\text{area}}$ would follow the shape of noise granularity function provided the circle diameters are large relative to the point spread function of the imaging system. However, there is evidence[2] that this may not be the case for similated CT noise.

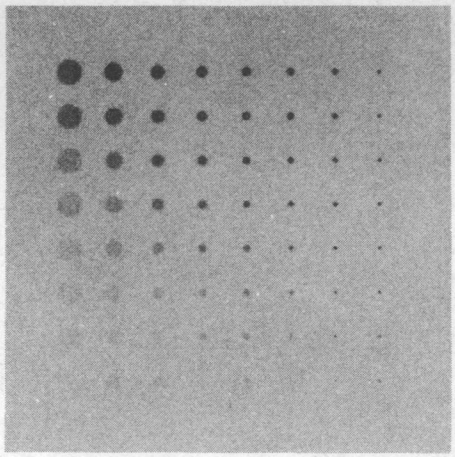

Figure 6

The detectability pattern. The circle diameters decrease by a factor of $\sqrt{2}$ from column to column. In each row the product of contrast times diameter remains constant while this product decreases by $\sqrt{2}$ in going from one row to the next.

- - - - - - - -

A detectability phantom has been constructed which when imaged by x rays will produce the detectability pattern shown in Figure 6. It consists of a plexiglas (lucite) base with a pattern of holes filled with aqueous K_2HPO_4 solutions. The hole diameters ranged from 2 to 16 mm in $\sqrt{2}$ steps. The strongest solution was made by dissolving 80 gm of K_2HPO_4 in 1 liter of water. The solutions are weakened by factors of $\sqrt{2}$ to obtain variable contrast. The phantom is mounted inside a water bath with a 25.4 cm diameter. This phantom has been scanned by an EMI 5005 with the x-ray tube voltage adjusted to 90 kV in order to reduce the contrast of the strongest K_2HPO_4 solution (bottom large hole in Fig. 6) to essentially zero. The resulting slow (70 sec) scan is shown in Figure 7a. The smallest hole (2 mm) on the top row contains the weakest solution and has a contrast of above 56 CT numbers (11.2%) relative to the plexiglas. The largest hole (16 mm) on the top row has a contrast of 7 CT numbers (1.4%). The noise levels in this CT image are about 2.8 times larger than they would be for a normal scan at 140 kV. It should be noted that in the normal full size EMI display spatial smoothing is carried out on the 320 x 320 data matrix to obtain the 160 x 160 display matrix. Figure 7b shows a fast scan of the same phantom at the same technical factors in which the image has been filtered using a Hanning filter whose half value occurs at 1/8 the Nyquist frequency (based on the 320 x 320 matrix). It is observed that the detectability of the larger circles is nearly the same as in Figure 7a even though the noise level in the fast scan is a factor of two larger than in the slow scan. It has previously been found[2] in simulated CT

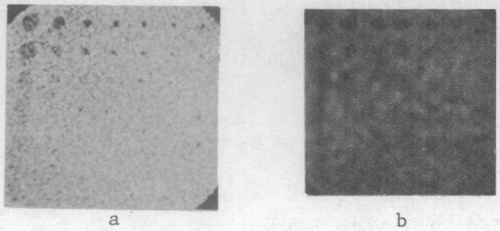

a b

Figure 7

Two scans of the detectability phantom by the EMI 5005 at 90 kVp.
(a) A normal display of a slow (70 sec) scan.
(b) A smoothed display of a fast (22 sec) scan.

- - - - - - -

reconstructions that under certain circumstances human observers' detection capabilities of large circles are enhanced through the use of spatial smoothing. This should be investigated further with images from CT scanners.

Conclusions

It has been shown that the EMI 5005 scanner produces images with noise characteristics similar to those in simulated CT reconstructions. A detectability phantom has been described which will provide a means of investigation of the effect on human detection capability of the peculiar correlations present in the noise present in CT scanner images.

References

1. Riederer, S.J., Pelc, N.J. and Chesler, D.A., "Statistical Aspects of Computed X-Ray Tomography", presented at 4th Int. Conf. on Medical Physics, Ottawa, Canada, 1976 and submitted to Phys. Med. Bio.

2. Hanson, K.M., "Detectability in the Presence of Computed Tomographic Reconstruction Noise", presented at the SPIE/SPSE Conf. on Appl. of Op. Instr. in Medicine VI, Sept. 1977, Boston, MA and to be published in the Proceedings of the Photo-Optical Instrumentation Engineers.

3. Boyd, D.P., Korobkin, M.T. and Moss, A., Proc. of SPIE, Appl. of Op. Instr. in Medicine V, Vol. 96, 303-312 (1976).

4. Frieser, H., Phot.Sc. Eng. 3, 223-228 (1959).

5. Burger, G.C.E., Philips Tech Rev., Vol. 11, pp. 291 (1950).

6. Rosell, F.A. and Willson, R.H., Perception of Displayed Information, Lucien M. Biberman, ed., Plenum Press New York 1973.

Acknowledgements

We would like to thank Peter Berardo and Sandra Zink for transcribing the EMI tapes and Bernard Hruska for contructing the detectability phantom.